

not in ml
" " LL

R

CONTRACTOR REPORT

SAND86-7005
Unlimited Release
UC-70

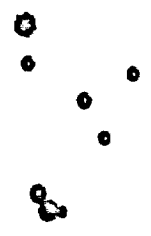
Nevada Nuclear Waste Storage Investigations Project

Reference Thermal and Thermal/Mechanical Analyses of Drifts for Vertical and Horizontal Emplacement of Nuclear Waste in a Repository in Tuff

C. M. St. John
J.F.T. Agapito and Associates, Inc.
27520 Hawthorne Blvd., Suite 295
Rolling Hills Estates, CA 90274

Prepared by Sandia National Laboratories, Albuquerque, New Mexico 87185
and Livermore, California 94550 for the United States Department of Energy
under Contract DE-AC04-76DP00789

Printed May 1987



SAND86-7005

Unlimited Release
Printed May 1987

REFERENCE THERMAL AND THERMAL/MECHANICAL ANALYSES OF DRIFTS FOR
VERTICAL AND HORIZONTAL EMPLACEMENT OF NUCLEAR
WASTE IN A REPOSITORY IN TUFF

by

C.M. St. John

J.F.T. Agapito and Associates, Inc.
27520 Hawthorne Blvd., Suite 295
Rolling Hills Estates, CA 90274

for

Sandia National Laboratories
P. O. Box 5800
Albuquerque, New Mexico 87185

Under Sandia Contract: 25-8908

Sandia Contract Monitor
B. Ehgartner
Geotechnical Design Division 6314

ABSTRACT

Two-dimensional thermal and thermal/mechanical analyses of the designs of drifts for vertical and horizontal emplacement of nuclear waste in a repository in tuff were performed using boundary-element and finite-element computer codes. The finite-element analyses considered the two extreme alternatives of continuous ventilation for 100 yr after waste emplacement and that of no ventilation at any time. The boundary-element code was utilized during scoping studies and it also provided independent verification of the results of the finite-element analyses. The analyses predict the development of increased horizontal stress levels in the rock mass as a result of waste emplacement. These are moderated significantly by ventilation in the case of vertical emplacement, because the drifts are spaced sufficiently close for a substantial amount of the heat generated by the waste to be removed by the ventilating air. Even without such a moderating influence, there is no evidence that the stresses induced by waste emplacement would lead to drift instability. For none of the cases considered was there any indication of a potential for failure of the rock matrix. Regions of overstress of joints were predicted in all cases, but such regions were small and are judged to be of little or no practical significance to the stability of the emplacement drift.

ACKNOWLEDGEMENTS

This study was initiated by Brian Ehgartner, who played an active role in task definition, analysis, and final report preparation. Rex Goodrich was responsible for the finite-element analyses of the ventilated emplacement drifts, and he completed the code modifications necessary for preparing many of the plots contained within the report. Kandiah Arulmoli subsequently modified the finite-element models for the unventilated drifts and performed those analyses. He also completed the series of boundary-element analyses.

TABLE OF CONTENTS

ACKNOWLEDGEMENTS

<u>Section</u>		<u>Page</u>
1.	INTRODUCTION	
	1.1 Purpose and Justification	1
	1.2 Approach	1
	1.3 Assumptions	2
2.	PROBLEM DEFINITION	
	2.1 General Description	2
	2.2 Vertical Emplacement	3
	2.3 Horizontal Emplacement	4
	2.4 Rock Mass Properties	6
	2.5 Waste Characteristics	6
3.	ANALYTICAL APPROACH	
	3.1 Introduction	7
	3.2 Boundary-Element Analysis	8
	3.2.1 The Computer Code	8
	3.2.2 The Numerical Models	9
	3.2.3 Strength of Heat Sources	9
	3.2.4 Investigation of Repository Model	10
	3.3 Finite-Element Analysis	12
	3.3.1 The Computer Codes	12
	3.3.2 The Numerical Models	13
	3.4 Approximations for Ventilated and Unventilated Drifts	14
	3.5 Methods of Stability Evaluation	15
4.	ANALYSIS RESULTS	
	4.1 Vertical Emplacement	17
	4.2 Horizontal Emplacement	20
5.	DISCUSSION	21
	REFERENCES	25
	APPENDICES	
	A - BOUNDARY-ELEMENT ANALYSES OF VERTICAL EMPLACEMENT	
	B - FINITE ELEMENT-ANALYSES OF VERTICAL EMPLACEMENT	
	C - BOUNDARY-ELEMENT ANALYSES OF HORIZONTAL EMPLACEMENT	
	D - FINITE-ELEMENT ANALYSES OF HORIZONTAL EMPLACEMENT	
	E - MEMO: Mansure, A.J., "Allowable Thermal Loading as a Function of Waste Age."	
	F - MEMO: Mansure, A.J. and R.E. Stinebaugh, "Memorandum of Record of Instructions for Thermal Design, Analysis, and Performance Assessment of Layout, Version 1."	
	G - COMPARISON OF STUDY DATA WITH NNWSI REFERENCE INFORMATION BASE	
	H - DISTRIBUTION LIST	

LIST OF FIGURES

<u>Figure</u>		<u>Page</u>
1	Design of Drift for Vertical Emplacement of Waste Container of Spent Fuel	38
2	Design Module of Vertical Emplacement Panels	39
3	Design of Drift for Horizontal Emplacement of Waste Container of Spent Fuel	40
4	Design Module of Horizontal Emplacement Panels	41
5	Boundary-Element Model for Analysis of Vertical Emplacement (a) Complete (b) Drift Detail and Sample Points	42
6	Boundary-Element Model for Analysis of Horizontal Emplacement (a) Complete (b) Drift Detail and Sample Points	43
7	Thermally Induced Stresses in the Plane of a Single Panel 100 Yr After Waste Emplacement in Horizontal Boreholes	44
8	Finite-Element Model for Analysis of Vertical Emplacement (a) Complete Mesh (b) Details of Mesh around Drift	45
9	Finite-Element Model for Analysis of Horizontal Emplacement (a) Complete Mesh (b) Details of Mesh around Drift	46
10	Boundary-Element Predictions of Wall Temperatures of the Vertical Emplacement Drift - Unventilated Drift	47
11	Boundary-Element Predictions of Vertical and Horizontal Closures of the Vertical Emplacement Drift - Unventilated Drift	48
12	Boundary-Element Predictions of Tangential Stresses at Selected Points Around the Vertical Emplacement Drift - Unventilated Drift	49
13	Boundary-Element Predictions of Principal Stresses in the Vicinity of the Vertical Emplacement Drift - Unventilated Drift	50
14	Boundary-Element Predictions of Tangential Stress Distribution Around the Vertical Emplacement Drift - Unventilated Drift	51
15	Boundary-Element Predictions of the Ratio Between the Matrix Strength and Stress Around the Vertical Emplacement Drift - Unventilated Drift	52
16	Boundary-Element Predictions of the Ratio Between the Joint Strength and Stress Around the Vertical Emplacement Drift - Unventilated Drift	53
17	Finite-Element Predictions of the Temperature Change in the Vicinity of the Vertical Emplacement Drift 100 Yr After Waste Emplacement	54

LIST OF FIGURES

<u>Figure</u>		<u>Page</u>
18	Finite-Element Predictions of the Principal Stresses in the Vicinity of the Vertical Emplacement Drift	55
19	Finite-Element Predictions of the Ratio Between Matrix Strength and Stress Around the Vertical Emplacement Drift	56
20	Finite-Element Predictions of the Ratio Between Joint Strength and Stress Around the Vertical Emplacement Drift	57
21	Boundary-Element Predictions of the Ratio Between Joint Strength and Stress Around an Unventilated Vertical Emplacement Drift, at Times up to 100 Yr After Waste Emplacement	58
22	Boundary-Element Predictions of Wall Temperatures of the Horizontal Emplacement Drift - Unventilated Drift	59
23	Boundary-Element Predictions of Vertical and Horizontal Closures of the Horizontal Emplacement Drift - Unventilated Drift	60
24	Boundary-Element Predictions of Tangential Stresses at Selected Points Around the Horizontal Emplacement Drift - Unventilated Drift	61
25	Boundary-Element Predictions of Principal Stresses in the Vicinity of the Horizontal Emplacement Drift - Unventilated Drift	62
26	Boundary-Element Predictions of Tangential Stress Distribution Around the Horizontal Emplacement Drift - Unventilated Drift	63
27	Boundary-Element Predictions of the Ratio Between the Matrix Strength and Stress Around the Horizontal Emplacement Drift - Unventilated Drift	64
28	Boundary-Element Predictions of the Ratio Between the Joint Strength and Stress Around the Horizontal Emplacement Drift - Unventilated Drift	65
29	Finite-Element Predictions of the Temperature Changes in the Vicinity of the Horizontal Emplacement Drift 100 Yr After Waste Emplacement	66
30	Finite-Element Predictions of the Principal Stresses in the Vicinity of the Horizontal Emplacement Drift	67
31	Finite-Element Predictions of the Ratio Between Matrix Strength and Stress Around the Horizontal Emplacement Drift	68
32	Finite-Element Predictions of the Ratio Between Joint Strength and Stress Around the Horizontal Emplacement Drift	69
33	Comparison of Closure Histories For the Drift with No Ventilation, Computed Using Boundary-Element and Finite-Element Models: Vertical Emplacement	70

LIST OF FIGURES

<u>Figure</u>		<u>Page</u>
34	Comparison of Closure Histories for the Drift With No Ventilation, Computed Using Boundary-Element and Finite Element Models: Horizontal Emplacement	71
35	Temperature Histories for Points in the Interior of the Rock Mass.	72
36	Approximate Histories of the Horizontal Stresses to which the Waste Emplacement Drifts are Subjected.	73
37	Conceptual Interpretation of the Development of Regions in which the Shear Stress on Vertical Joints Exceeds their Shear Strength	74

LIST OF FIGURES

APPENDIX A

<u>Figure</u>		<u>Page</u>
A.1	Boundary-Element Predictions of Principal Stresses in the Vicinity of the Vertical Emplacement Drift, at Times up to 100 Yr After Waste Emplacement - Unventilated Drift	A-2
A.2	Boundary-Element Predictions of Tangential Stress Distribution Around the Vertical Emplacement Drift, at Times up to 100 Yr After Waste Emplacement Unventilated Drift	A-3
A.3	Boundary-Element Predictions of the Ratio Between the Matrix Strength and Stress Around the Vertical Emplacement Drift, at Times up to 100 Yr After Waste Emplacement - Unventilated Drift	A-4
A.4	Boundary-Element Predictions of the Ratio Between the Joint Strength and Stress Around the Vertical Emplacement Drift, at Times up to 100 Yr After Waste Emplacement - Unventilated Drift	A-5

LIST OF FIGURES

APPENDIX B

<u>Figure</u>		<u>Page</u>
B.1	Finite-Element Prediction of Deformations in the Vicinity of the Vertical Emplacement Drift, at Times up to 100 Yr After Waste Emplacement	
	(a) Unventilated Case	B-2
	(b) Ventilated Case	B-3
B.2	Finite-Element Predictions of the Temperature Changes (°C) in the Vicinity of the Vertical Emplacement Drift, at Times up to 100 Yr After Waste Emplacement	
	(a) Unventilated Case	B-4
	(b) Ventilated Case	B-5
B.3	Finite-Element Predictions of the Principal Stresses in the Vicinity of the Vertical Emplacement Drift, at Times up to 100 Yr After Waste Emplacement	
	(a) Unventilated Case	B-6
	(b) Ventilated Case	B-7
B.4	Finite-Element Predictions of the Ratio Between Matrix Strength and Stress Around the Vertical Emplacement Drift, at Times up to 100 Yr After Waste Emplacement	
	(a) Unventilated Case	B-8
	(b) Ventilated Case	B-9
B.5	Finite-Element Predictions of the Ratio Between Joint Strength and Stress Around the Vertical Emplacement Drift, at Times up to 100 Yr After Waste Emplacement	
	(a) Unventilated Case	B-10
	(b) Ventilated Case	B-11

LIST OF FIGURES

APPENDIX C

<u>Figure</u>		<u>Page</u>
C.1	Boundary-Element Predictions of Principal Stresses in the Vicinity of the Horizontal Emplacement Drift, at Times up to 100 Yr After Waste Emplacement - Unventilated Drift	C-2
C.2	Boundary-Element Predictions of Tangential Stress Distribution Around the Horizontal Emplacement Drift, at Times up to 100 Yr After Waste Emplacement - Unventilated Drift	C-3
C.3	Boundary-Element Predictions of the Ratio Between the Matrix Strength and Stress Around the Horizontal Emplacement Drift, at Times up to 100 Yr After Waste Emplacement - Unventilated Drift	C-4
C.4	Boundary-Element Predictions of the Ratio Between the Joint Strength and Stress Around the Horizontal Emplacement Drift, at Times up to 100 Yr After Waste Emplacement - Unventilated Drift	C-5

LIST OF FIGURES

APPENDIX D

<u>Figure</u>		<u>Page</u>
D.1	Finite-Element Prediction of Deformations in the Vicinity of the Horizontal Emplacement Drift, at Times up to 100 Yr After Waste Emplacement.	
	(a) Unventilated Case	D-2
	(b) Ventilated Case	D-3
D.2	Finite-Element Predictions of the Temperature Changes ($^{\circ}$ C) in the Vicinity of the Drift for the Horizontal Emplacement Drift, at Times up to 100 Yr After Waste Emplacement -	
	(a) Unventilated Case, in the Vicinity of the Drift	D-4
	(b) Unventilated Case, in the Far-Field	D-5
	(c) Ventilated Case, in the Vicinity of the Drift	D-6
	(d) Ventilated Case, in the Far-Field	D-7
D.3	Finite-Element Predictions of the Principal Stresses in the Vicinity of the Horizontal Emplacement Drift, at Times up to 100 Yr After Waste Emplacement	
	(a) Unventilated Case	D-8
	(b) Ventilated Case	D-9
D.4	Finite-Element Predictions of the Ratio Between Matrix Strength and Stress Around the Horizontal Emplacement Drift, at Times up to 100 Yr After Waste Emplacement	
	(a) Unventilated Case	D-10
	(b) Ventilated Case	D-11
D.5	Finite-Element Predictions of the Ratio Between Joint Strength and Stress Around the Horizontal Emplacement Drift, at Times up to 100 Yr After Waste Emplacement	
	(a) Unventilated Case	D-12
	(b) Ventilated Case	D-13

LIST OF TABLES

<u>Table</u>		<u>Page</u>
1	Geometric Data for Vertical Emplacement Option	27
2	Geometric Data for Horizontal Emplacement Option	28
3	Data for Thermal and Thermal/Mechanical Analyses of Emplacement Drifts	29
4	Normalized Coefficients for the Power Decay Function for PWR and BWR Spent Fuel Mix	30
5	Results of Preliminary Analyses of the Horizontal Emplacement Option -- Data For 100 Yr After Emplacement	31
6	Thermal Analyses Performed Using the DOT Computer Code	32
7	Results of Thermal Analyses of Unventilated Vertical Emplacement Drift Using Alternative Effective Thermal Conductivities	33
8	Results of Boundary-Element Analyses of the Vertical Emplacement Drift	34
9	Results of Finite-Element Analyses of the Vertical Emplacement Drift	35
10	Results of Boundary-Element Analyses of the Horizontal Emplacement Drift	36
11	Results of Finite-Element Analyses of the Horizontal Emplacement Drift	37

LIST OF TABLES

APPENDIX G

<u>Table</u>		<u>Page</u>
G.1	Material Property Data	G-2
G.2a	Geometric Data for Vertical Emplacement Option	G-3
G.2b	Geometric Data for Horizontal Emplacement Option	G-4

1. INTRODUCTION

1.1 Purpose and Justification

The work described in this report was performed for Sandia National Laboratories (SNL) as a part of the Nevada Nuclear Waste Storage Investigations (NNWSI) project. Sandia is one of the principal organizations participating in the project, which is managed by the U.S. Department of Energy's Nevada Operations Office (DOE-NV). The project is part of the Department of Energy's program to develop methods for safe disposal of the radioactive waste from nuclear power plants.

The DOE has determined that the safest and most feasible method currently known for the disposal of such waste is to emplace it in mined geologic repositories. The NNWSI project is conducting detailed studies of an area on and adjacent to the Nevada Test Site (NTS) in southern Nevada to determine the feasibility of developing a repository at that location.

This report documents the results of a numerical investigation of the thermal and thermal/mechanical behavior of a tuff rock mass around emplacement drifts within typical waste-isolation panels of a nuclear waste repository. The purpose of the study was to provide a consistent set of predictions of the conditions anticipated in and around emplacement drifts for the two radioactive waste emplacement options currently being considered: namely, vertical emplacement and horizontal emplacement. The analyses were performed using the best current estimates of the rock mass properties and waste characteristics, and geometric data obtained from a preliminary design for a repository at the candidate site at Yucca Mountain, in Southern Nevada. That design differs in some respects from the current conceptual design for the repository. However, the results of the analyses presented herein never-the-less provide a basis for evaluating the adequacy of the current, conceptual design of emplacement drifts. They also provide a part of the basis for evaluating the feasibility of retrieval of the waste, for evaluating non-radiological safety concerns during repository operations, and serve to help verify computer codes by comparing independent sets of calculations. In addition, the analyses provide some insight into sensitivity of the results to proximity of adjacent waste panels and to differences in emplacement orientation. Other drift designs, or alternative waste-emplacement methods, could be analyzed in the same manner as described in this report.

1.2 Approach

Simple configurations were developed for the repository site and for drifts that would be excavated for vertical and horizontal emplacement of waste containers. Thermal and thermal/mechanical analyses were then performed for the simplified configurations using boundary-element and finite-element codes. The boundary-element analyses approximated an unventilated drift, whereas the finite-

element analyses explicitly considered the extreme alternatives of continuous ventilation and no ventilation. Direct comparison between the two analytical methods was possible for the case of mechanical loading only (i.e. before ventilation or waste emplacement). The results of the thermal/mechanical analyses were subsequently processed to develop plots of temperature, deformation, and stress. In addition, plots of the ratio of computed stress to estimated strength were prepared for the rock matrix and for vertical joints assumed to pre-exist within the rock mass.

1.3 Assumptions

Repository layout, drift geometries, waste characteristics, rock mass thermal and thermal/mechanical properties, and other data used for analyses described in this report are discussed in detail in Section 2. However, it is worth noting that the analyses are based on three assumptions. These are, first, that the rock mass within which the repository is constructed is homogeneous and linearly elastic; second, that material properties characterizing the rock mass are independent of time and any changes in temperature or moisture content; and third, that it is sufficient to model a two-dimensional cross section of the simplified repository layout. Review of the results presented in this report indicate that the assumption of linearly elastic behavior is a reasonable approximation, and the predicted range of temperatures around the drifts is one over which mechanical and thermal mechanical properties are reported to be constant (Zeuch and Eatough, 1986). The assumption that material properties are independent of time is consistent with the current understanding of the mechanical behavior of tuff over the stress and temperature ranges of concern (Section 2.3.1, Site Characterization Plan, DOE, in preparation). Justification of the simplifying assumptions of homogeneity and a two-dimensional geometry are provided below.

2. PROBLEM DEFINITION

2.1 General Description

The nuclear waste repository discussed in this report is assumed to comprise a number of contiguous panels within which waste is emplaced, from specially prepared emplacement drifts, into either vertical or horizontal emplacement holes. The actual distribution of such panels is dependent upon a number of considerations, including physical limitations imposed by the site and the location of any shafts, ramps, and other underground facilities necessary to repository operation. Such details may be considered during site performance assessment, but because of the localized scale of interest are not critical to an analysis of the behavior of a typical waste-emplacement drift within the repository. For the same reason the details of the surface topography and stratigraphy of regions substantially above and below the drifts can be neglected.

If the specifics of the repository layout, surface topography, and stratigraphy are ignored, the repository can be idealized as several adjacent panels located at some depth in a homogeneous rock mass with a horizontal ground surface. In the present instance the waste-emplacement panels described in Subsections 2.2 and 2.3 were assumed to be located at an average depth of 302 m below the surface. The rock mass was uniformly ascribed the properties of the stratigraphic member currently considered as the candidate for waste emplacement. This simplification was justified on two counts. First, because the candidate member is relatively thick, it has the greatest influence on the overall response of the rock mass to waste emplacement. Second, this study was intended to provide predictions of temperatures, displacements, and stresses around the waste-emplacement drifts. These are most influenced by the properties of the rock mass within which the drifts are excavated.

As noted, no attempt was made to model the layout of an actual repository. Instead, two-dimensional analyses of the cross section of typical emplacement drifts, 302 m below a plane horizontal surface, were performed. It was assumed that there would be no deformation normal to the plane of the cross section, which is equivalent to assuming that the emplacement drifts are infinitely long, or at least long enough for plane strain conditions to be applicable. The results of analyses are, therefore, representative of conditions within all but the outer edges of an emplacement panel. In the boundary-element calculations the repository was assumed to be about 1,300 m wide. The predicted conditions would thus be typical of an emplacement drift within a large but finite repository. In contrast, the finite-element calculations assumed two lines of symmetry: one at the center of the emplacement drifts and the other midway between adjacent drifts. When coupled with the condition that there will be no deformation normal to the plane of the cross section, these symmetries are equivalent to assuming that the repository is of infinite areal extent. The predicted conditions will thus be typical of an emplacement drift inside a large repository and may be more severe than would be encountered in practice. Since the drifts in the current repository designs are long, in comparison to their width, and since it was the objective of these reference calculations to establish the response of typical drifts in the repository these simplified models of the repository are considered acceptable.

2.2 Vertical Emplacement

In the vertical emplacement option currently being considered, single waste containers are emplaced in short vertical holes drilled into the floor of the waste-emplacement drifts. Figure 1 illustrates the current design concept and dimensions for such drifts (Parsons, Brinckerhoff, Quade, & Douglas, 1985). The dimensions given in that figure are largely dictated by present design concepts for a vehicle that would transport waste containers to the emplacement drifts in shielded casks. Drift height is determined by the length of the container (approximately 4-5 m) plus the shielding needed for the transporter cask

plus the amount of clearance desired between the roof and the cask during emplacement. Unless the design concepts for the waste transporter or container change significantly, the height of the drift is unlikely to change greatly.

In the vertical emplacement option the containers are emplaced in a single line down the center of the floor of the drifts. In the current design concepts the emplacement panels consist of several parallel emplacement drifts and the associated access drifts. One design module of a typical emplacement panel is illustrated in Figure 2 (Mansure and Stinebaugh, 1985 - refer to Appendix F). The dimensions of that module are determined by the panel width and the emplacement-drift spacing. The panel width and the emplacement-drift spacing are related to the spacing of containers in the drift floor, the thermal output of individual containers, and the average thermal loading of the panel. Specifically, the relationship between areal power density (APD) and the other parameters for the design module is as follows.

$$APD = \frac{CHO \cdot m}{x \cdot w}$$

in which CHO = waste container heat output,
m = number of containers per module,
x = drift spacing, and
w = panel width.

The values of the parameters required to define the design for vertical emplacement, which was analyzed during this study, are summarized in Table 1, and the drift geometry is illustrated in Figure 1. For comparison purposes, the dimensions used in the current conceptual design are also given in the table. Note that only the parameters APD, x, and w are defined in Table 1. These were used to calculate the total heat load of each emplacement drift (CHO·m) and, hence, the thermal loading per unit length of the drift.

The present study was based on the assumption that waste would be emplaced to achieve an average initial thermal loading density (APD) of 57 kW/acre (14.1 W/m²) within the design module. That figure is equivalent to a total initial thermal load of 205.18 kW per module. Neither the number of containers nor the individual container heat output were explicitly considered. However, consideration was given to the fact that there is a standoff between the access drifts and the first borehole in each emplacement drift. Figure 2 and Table I indicate that containers are actually concentrated within the central 1.140 ft (347.47 m) of the emplacement drift, thereby achieving a local thermal loading density of 590.5 W/m of drift.

2.3 Horizontal Emplacement

In the horizontal emplacement option currently being considered, the waste containers are placed in long holes drilled horizontally from both sidewalls of

the emplacement drifts. The span of these drifts needs to be much greater than those for vertical emplacement, because the container and its shielding cask must be positioned across the drift for container emplacement in the horizontal holes. However, in the design analyzed, a reduced span is used over most of the length of the drift with a local enlargement, or alcove, at each emplacement borehole. The dimensions of the drift sections between the emplacement alcoves are illustrated in Figure 3 (Parsons, Brinckerhoff, Quade, and Douglas, 1985). In the current conceptual design the alcoves have been eliminated, and emplacement drifts are the same span over their entire length.

A waste-emplacement panel for horizontal emplacement comprises a single emplacement drift from which a number of parallel emplacement boreholes are drilled. Because many containers are emplaced in each hole, the spacing of drifts is much greater than for horizontal emplacement. Hence, description of the design module, which is illustrated in Figure 4, focusses on the emplacement holes rather than the drift, and the dimensions of the module are determined by the panel width and the emplacement borehole spacing. The relationship between the areal power density (APD) and the other parameters for the module is as follows.

$$APD = \frac{2 \cdot CHO \cdot n}{y \cdot w}$$

- in which CHO = waste container heat output,
- n = number of containers per emplacement hole,
- y = hole spacing, and
- w = panel width.

The values of the parameters required to define the design for horizontal emplacement that was analyzed during this study are summarized in Table 2. As for the vertical emplacement case the corresponding data for the current conceptual design has been included in the table for reference. Note that only the parameters APD, y, and w are defined in Table 2. These were used to calculate the total heat load of each emplacement borehole (CHO·n) and, hence, the thermal loading per unit length of borehole.

For the horizontal emplacement option an average thermal loading density of 57 kW/acre (14.1 W/m²) was again assumed for the design module. In this case, the total thermal loading of each design unit is 186.86 kW, which is equivalent to a thermal load of 528.50 W/m within the portion of the emplacement boreholes

$$14.1 = \frac{170 \cdot w}{31.09 \cdot 426.7}$$

$$140 \cdot w = 187000$$

$$\frac{187000}{426.7 - 35 \cdot 35} = 528 \frac{W}{m}$$

$$\frac{528}{31}$$

$$= 17 \frac{W}{m}$$

spacing borehole

occupied by waste containers. For a two-dimensional analysis of the emplacement drift, the thermal loading must be assumed to be distributed uniformly in a plane defined by the axes of the boreholes rather than concentrated along individual boreholes. Because emplacement boreholes are 102 ft (31.09 m) apart, an average thermal load of 17 W/m^2 (i.e., 17 w per meter of borehole per meter of drift) is calculated for the sections of the borehole in which waste is emplaced.

2.4 Rock Mass Properties

In the NNWSI program considerable attention has been devoted to the development of a common set of data to be used in geotechnical design and performance assessment calculations. As far as possible, these data are based on the results of laboratory and field measurements. However, there are instances in which site-specific data are not yet available. In such cases, recommended values have been developed on the basis of data from relevant sources and engineering judgment.

The recommended values for the matrix and the rock mass properties for the Yucca Mountain site are summarized in the NNWSI Reference Information Base (Zeuch and Eatough, 1986). These data comprise the average and the expected range for all stratigraphic members at Yucca Mountain. It is anticipated that a repository would be constructed in the lithophysae-poor, welded, devitrified tuff of the Topopah spring member. Table 3 lists average values for that unit. Data on other stratigraphic members present in Yucca Mountain are not reported here because the rock mass was modeled as homogeneous with properties equal to those of the candidate member.

Other data listed in Table 3 pertain to the temperature and stress before disturbance by repository construction and waste emplacement. Because the rock mass was assumed to be homogeneous, the vertical gradients of the temperature and the vertical stress are constant. At present there are very limited data on the horizontal stresses at the Yucca Mountain site. The ratio of horizontal to vertical in-situ stress quoted in Table 3 is in the middle of the range of 0.3 to 0.8, as recommended by Bauer, Holland, and Parrish (1985), who base their assessment on limited field measurements, finite-element analysis of topographical influences, and interpretation of the tectonic setting.

2.5 Waste Characteristics

The amount of thermal energy input into the host rock as a consequence of emplacement of high-level nuclear waste is governed by three design parameters: specifically, waste type, waste age, and emplacement density. The waste type actually emplaced within a repository will depend upon the inventory of waste fuel from nuclear reactors as well as national policy with respect to whether or not the waste is reprocessed before geologic isolation. For the purposes of this study it was assumed that the waste will consist of a mixture of unprocessed

spent fuel, with 60% of it from Pressurized Water Reactors (PWR) and 40% from Boiling Water Reactors (BWR).

The heat generated by nuclear waste is governed by the decay of the radioactive materials that comprise it. Predictions of the heat generation of a mixture of PWR and BWR spent fuel were taken from ORIGEN2 computer calculations done as a supplement to Appendix B of the DOE document entitled "Generic Requirements for a Mined Geologic Disposal System," (DOE, 1984). For geotechnical analyses, such as described herein, it is convenient to approximate the predicted heat generation, or power, by an equation of the following form.

$$P(t) = \sum_{i=1}^n a_i \exp(-b_i t),$$

in which $P(t)$ is the instantaneous power at t years relative to some time datum (such as removal from the nuclear reactor), and a_i and b_i are constants for the n exponential terms needed to adequately fit the data.

The number of terms required to fit the waste decay data is influenced by the period over which the fit is intended to be valid. The parameters for a four-component fit, valid for waste 5-500 yr out of the reactor, are reproduced in Table 4 (Mansure, 1985 - refer to Appendix E). For the purposes of the present study it was assumed that the waste will have been out of the reactor for 8.55 yr before emplacement within the repository. If emplacement time, rather than the time of the removal of the waste from the reactor is used as the time datum, the second set of coefficients given in Table 4 is used. For both sets of coefficients the power functions have been normalized to define unit power generation at the time datum. The actual power generation of the emplaced waste is calculated by multiplying the normalized value by the emplacement density, whether it be on the scale of a single waste container or averaged over an entire waste-emplacement panel.

3. ANALYTICAL APPROACH

3.1 Introduction

This section of the report presents a discussion of the numerical models used to obtain the results presented in Section 4 and in Appendices A through D. First, the analytical tools are described briefly, and the numerical models of the vertical and horizontal emplacement configurations are defined. Second, the approximations adopted for simulation of ventilated and unventilated drifts are discussed. Finally, the strength models used to assess the stability of the rock in the vicinity of drifts are described.

Two completely independent numerical techniques were used to perform analyses of the emplacement drifts; these were the boundary-element method and the finite-element method. This seeming redundancy served two purposes. First,

analysis by two independent methods ensured identification of any inconsistencies in the computer codes and in the numerical description of the repository and the drift. Second, it provided an excellent opportunity for evaluating under what conditions it is appropriate to use the boundary-element code for analysis of repository excavations. The net effect is that increased confidence is gained in the results and in the area of applicability of the models.

3.2 Boundary-Element Analysis

3.2.1 The Computer Code

Scoping calculations and analyses of the emplacement drifts were performed using the HEFF boundary-element code (Brady, 1980). The code is intended for approximate thermal/mechanical analysis of simple linear systems that can be treated in two dimensions. It is based on an indirect formulation of the boundary-element method for stress analysis, with thermal stresses treated as additional, time-varying, boundary conditions. The temperature distribution and corresponding thermal stresses are computed using the closed-form solution for line heat sources in an infinite medium. The lines extend infinitely in and out of the plane of analysis, therefore, they appear as points in any two-dimensional sections that HEFF is used to analyze. No attempt is made to satisfy any temperature boundary conditions at surfaces within the medium, with the result that the temperature and thermal stress field will be overestimated in those cases where there are any heat losses at those surfaces. That will be the case if an underground excavation in heated rock is cooled by ventilating air.

As noted above, HEFF utilizes the closed form solution for a line heat source, for obtaining temperatures, thermally induced stresses, and displacements within an infinite isotropic medium. Through the use of the method of images (Davis and DeWiest, 1966) it is possible to define a single plane of vertical symmetry and an isothermal horizontal surface, which represents the ground surface. The vertical line of symmetry automatically satisfies both thermal and mechanical boundary conditions. In contrast, the isothermal, horizontal surface 'created' by the method of images does not satisfy the mechanical boundary condition that the ground surface be free of shear tractions. The shear tractions on the surface must be 'removed' by adding boundary elements, with the boundary condition that they are free from both shear and normal traction.

HEFF is documented in a user's guide and manual (Brady, 1980), and examples of its application for analysis of underground excavations are contained in SAND83-7451 (St. John, 1983). The code documentation includes comparisons between the results of analyses using the HEFF code and the closed form solution for a circular hole in an elastic plate and finite-element analyses of an excavation in a heated rock mass. Verification of the thermal stress calculations within HEFF is discussed in detail by Lindner, St. John and Hart (1984). Crouch

and Starfield (1983) provide a detailed discussion and verification of the code upon which HEFF is based.

3.2.2 The Numerical Models

The two boundary-element models used to obtain results presented in Section 4 and Appendices A and C are illustrated in Figures 5 and 6. Temperatures, stress, and displacements were calculated at the midpoints of all boundary elements and also at the sample points marked in Figures 5b and 6b. For both the vertical and horizontal emplacement drifts, 26 boundary elements, plus a short element in the lower corner of the drift, were used to define one half of the drift perimeter. This number was selected to be approximately twice the number of finite elements (see Subsection 3.3) around each drift, because stress is assumed to be constant along a boundary element but varies linearly along the edge of the finite elements used in this study. Accordingly, this selection should result in similar numerical accuracies for the two models.

In the case of vertical emplacement, the drifts are spaced approximately 34 m apart. The thermal loading associated with each drift is explicitly represented by a single line source, but only the central emplacement drift and the one adjacent to it were modeled, as mechanical interactions between drifts more than about four equivalent diameters apart will be small. In the case of horizontal emplacement, only the one drift was modeled, and the emplacement holes were simulated by distributing line sources in the plane defined by the boreholes. Analyses were performed for the time of excavation and 5, 10, 20, 35, 50, 100, 150, and 200 yr after waste emplacement. Selected data from these analyses is presented in Subsections 4.1 and 4.2 and Appendices A and C.

3.2.3 Strength of Heat Sources

When performing HEFF analyses, it is necessary to represent heat sources as a number of discrete line sources perpendicular to the plane of analysis. For example, in the case of vertical emplacement, thermal loading that is due to the row of containers in the floor can be approximated as one or more line sources with a total strength equivalent to the average thermal loading of the drift. Specifically, for an initial thermal loading of 590.5 W/m of drift, the total strength of the line sources in the floor of each vertical emplacement drift will be

$$\text{Strength} = \frac{Q_0}{\rho c} = \frac{590.5 \text{ W/m}}{2.25 \text{ J/cm}^3\text{K}} = 8,282.0 \text{ K}\cdot\text{m}^3/\text{yr/m},$$

in which Q_0 is the initial thermal input and ρ and c are the density and specific heat capacity of the tuff rock mass.

Generally, the effect of containers emplaced from the drifts of the repository can be adequately approximated by single line sources located along

the centerline of each row of containers in the repository model. A better approximation is required if temperatures and stresses are to be calculated for points close to the source. This is the case for the boundary-element model of the vertical emplacement drift. Hence, the line of containers in the floor of the vertical emplacement drift was represented by three equal-strength line sources approximately 3.8 m, 5.3 m, and 6.9 m below the centerline of the floor of the drift.

In the case of horizontal emplacement, line sources must be distributed along the heated length of the emplacement holes to represent a heated plane defined by the container boreholes. The strength of each of these sources will depend upon the average thermal loading of the borehole and the borehole spacing. For the calculations reported herein, 35 line sources perpendicular to the borehole axis, each with initial strength of $1,204.0 \text{ K}\cdot\text{m}^3/\text{yr}/\text{m}$, were assumed to be uniformly distributed along the thermally loaded sections (176.8 m long) of the long borehole on either side of the emplacement drift. This is equivalent to placing a line heat source at the center of each container in the panel.

3.2.4 Investigation of Repository Model

Because it is possible to define only one plane of vertical symmetry in the boundary-element models used here, it is necessary to select a lateral extent for a model of a nuclear waste repository. Specifically, either the heat generated in every panel of the repository must be represented explicitly, or sufficient sources must be added to simulate an arbitrarily large repository. The latter course is simple if temperatures alone are to be computed, because the closed form solution for the line source can be used to demonstrate that the influence of any heat source will be small if the condition $(R^2/4\kappa t > 4)$ is satisfied. (R is the distance of the heat source, κ is the thermal diffusivity, and t is the time). For the analyses discussed here, the thermal diffusivity of the tuff was assumed to be $29.03 \text{ m}^2/\text{yr}$. The above condition, thus, suggests that no significant temperature change will result during the first 100 yr if a source is more than 215 m distant. This means that the temperature in the vicinity of a drift, in the center of the waste-emplacement panels of the size discussed here (427 m), will not be significantly influenced by waste emplaced in adjacent panels. However, all waste within the panel should be explicitly represented.

No simple range-of-influence condition exists for thermal stresses, but numerical experimentation can be used to investigate the effect of an ever increasing number of sources. In the present instance, trial calculations were performed to determine the total initial stress and temperature increase at the center of a panel, under the simplifying assumption that there were no drifts excavated on the repository horizon. Selected results of three series of calculations for the horizontal emplacement option 100 yr after panel loading are reproduced in Table 5. The model designated "single panel" utilized 35 heat

sources to represent the containers within a single emplacement hole. For the model designated "extended panel," 12 widely spaced sources were used to represent the waste emplaced within approximately 400 m of the panel centerline (i.e., the total heated section is approximately 2 panels wide). For the model designated "3 panels," 10 heat sources were added to the single-panel model to represent the waste emplaced in the adjacent panel. Three different boundary conditions were considered for the ground surface. First, presence of a free surface was ignored altogether. Second, the ground surface was assumed to be isothermal, but no measures were taken to remove shear forces induced at the ground surface as a result of thermal loading. Third, the ground surface was assumed to be isothermal, and boundary elements were added to define a stress-free surface extending either 1,000 m or 2,000 m from the drift centerline. Similar models of the vertical emplacement could have been prepared, but this was considered unnecessary because differences between the two emplacement options are less significant when investigating large-scale responses for the entire repository than when analyzing the behavior of the emplacement drifts.

The data presented in Table 5 support the prediction that waste in adjacent panels will have an insignificant effect on the temperature of the rock near the drift. That the temperature for the extended panel case is lower than the others may be attributed to the use of fewer, more widely spaced sources in that model. The temperatures are also recognized as insensitive to the free surface condition.

The effect of adjacent panels and the ground surface on the stresses experienced at the drift in the center of the model is greater than the effect on the temperature. This is illustrated by the data listed in Table 5. In that table the total initial stresses are the sum of the initial values and the thermally induced stresses. The initial horizontal and vertical stresses at repository depth are, respectively, 3.82 MPa and 6.95 MPa. The effect of waste emplacement is a marked increase in the horizontal stress level, whereas the vertical stress level decreases. These effects are obviously influenced by both the number of heat sources and the extent of the ground surface that is modeled.

The influence of additional heat sources on the stresses deserves some additional explanation. In the immediate vicinity of a heat source, thermal expansion induces a compressive stress field. In the surrounding, cooler rock the induced radial stress will be compressive but the circumferential stress will be decreased. Shown in Figure 7 are plots of the induced stress 100 yr after waste emplacement: these predicted stresses are for a single horizontal emplacement panel. It may be observed that the induced vertical stress is compressive only in the immediate vicinity of the emplaced waste. In the center of the panel, where the rock mass is relatively cool because of the large standoff distance of the waste from the horizontal emplacement drift, the induced vertical stress is tensile. The same effect is observed at the outer edge of the panel. Figure 7 also illustrates that including the ground surface in the repository

reduces the peak vertical stress in the thermally loaded section of the panel and decreases the vertical stress in the center of the panel and at the panel boundary. This occurs because the introduction of the free surface allows the heated rock mass to expand upward without constraint. As might be anticipated, the effect of the free surface on the horizontal stress is much less marked.

Because the predicted temperatures and stresses are influenced by the number of heat sources included and by the extent of the ground surface modeled, any repository model must be chosen judiciously. In choosing the model geometry, the additional computational cost of a large model must be weighed against increased accuracy. Consideration also must be given to the fact that a real repository will not be of infinite extent. In the present case, the three-panel model was selected for all boundary-element analyses. The ground surface was modeled by boundary elements extending 1,000 m from the drift centerline, because the effect of additional surface elements had been demonstrated to be small. The results of analyses performed, using this model, should be very similar to those for an infinite model for at least the first 100 yr after waste emplacement, when the thermal disturbance of the site is small. Differences between the boundary-element and finite-element analyses reported herein will be due, at least in part, to real differences in the repository model. Other differences will be caused by the approximations of the thermal analyses in the boundary element model.

3.3 Finite-Element Analysis

3.3.1 Computer Codes

Analyses were performed with two finite-element computer codes, DOT and VISCOT, that are part of a group of performance-assessment codes developed and supported by the Office of Nuclear Waste Isolation (ONWI). DOT is a general-purpose, heat-conduction code for both linear and nonlinear steady-state or transient analysis. It was developed originally by Polivka and Wilson (1976) and subsequently adopted as one of ONWI's performance-assessment codes. It is documented in a technical report (ONWI-420) prepared by INTERA Environmental Consultants (ONWI, 1983a).

VISCOT is a general-purpose, nonlinear, transient, thermal/mechanical, two-dimensional, finite-element code designed to determine the elastic, viscoelastic, viscoplastic, or elastoplastic deformation of a rock mass due to mechanical and thermal loading. It is derived from the program VISCOUNT, which is described in the textbook Finite Elements in Plasticity: Theory and Practice (Owen and Hinton, 1980). Like DOT, it was adopted by ONWI as one of their performance-assessment codes and is documented in a technical report (ONWI-437) prepared by INTERA Environmental Consultants (ONWI, 1983b). Also like DOT, it allows the use of four- and eight-node, isoparametric, quadrilateral, finite elements in plane and axisymmetric geometries. This permits ready integration of the two codes

because they may share identical meshes, and nodal point temperatures computed by using DOT can be input directly into VISCOT as initial conditions for thermal/mechanical analysis.

3.3.2 The Numerical Models

The finite-element meshes used for analyses of the vertical and horizontal emplacement options are illustrated in Figures 8 and 9. A total of 145 second-order elements and 504 nodes was used in the idealization of the rock mass for the vertical-emplacement option, and 194 elements and 651 nodes, respectively, were used for the horizontal-emplacement method. For analysis of the unventilated drift, additional elements were used to model air within the drift; 25 were used in the vertical emplacement drift and 16 in the horizontal emplacement drift. Both meshes extended from the ground surface to a depth of 500 m, or approximately 200 m below the emplacement horizon, and utilize planes of symmetry at the centerline of the drift and midway between adjacent drifts. Similar mesh refinement is used in the vicinity of the two emplacement drifts to minimize the possible influence of that parameter during any comparison between the two alternative emplacement options.

Details of the transient thermal analyses of the ventilated and unventilated drifts that were performed using the DOT heat transfer code are summarized in Table 6. That table defines the number of time steps used to perform each of the calculations, the time step lengths, and the time increment for a linearized form of the power decay function. There were two important differences between the analyses of the vertical and horizontal emplacement drifts. First, because of the higher thermal gradients near the vertical emplacement drift, shorter time steps were used during analysis of that emplacement option. Second, in the case of vertical emplacement the heat generation was assumed to be uniform within a single element with a cross section approximately equal to that of a typical container (i.e., 4.5 m high and 0.74 m wide), but heat generation was concentrated at nodal points in the analysis of the horizontal emplacement drift.

For the vertical emplacement drift analysis, the heat-generating element was assumed to have thermal and mechanical properties identical to the host rock, because it was not the purpose of the analysis to examine container scale effects. For the horizontal emplacement drift analysis, heat flux equivalent to the power generated by the waste in the emplacement boreholes was prescribed at nodal points located in the plane defined by the borehole axes. To approximate uniform flux, the values assigned at mid-side nodes were weighted in the usual manner (i.e., the flux at mid-side nodes is weighted three times, relative to corner nodes; Zienkiewicz, 1977).

The purpose of the DOT analyses was to prepare nodal-point temperature distributions for input into the VISCOT code at 10, 35, and 100 yr after waste emplacement, these three times having been selected as representative after the

scoping calculations performed with the boundary-element models and to allow evaluation as to whether or not the retrieval option would be maintained over this period. VISCOT analyses were first performed for determining the conditions immediately after excavation and subsequently at the selected times, with the use of the computed temperature distribution as initial conditions. The results of these analyses are presented in Sections 4.1 and 4.2 and Appendices B and D.

3.4 Approximations for Ventilated and Unventilated Drifts

The finite-element code DOT was used to simulate the two alternative cases of ventilated and unventilated drifts, whereas the HEFF code provided an approximation for only the unventilated case. The HEFF boundary-element code does not make any provision for heat loss at any interior surfaces, such as occurs with ventilation of the drifts. In fact, the drift is not modeled during the thermal calculations, which utilize analytical solutions for heat sources in an infinite medium. Accordingly, HEFF provides a poor approximation of the behavior of the rock mass around a drift in which there is significant heat loss to a ventilation system. In contrast, the approximation for an unventilated drift can be relatively good, particularly if the temperature gradients in the vicinity of the drift are low. Horizontal emplacement satisfies the latter condition. However, in the case of vertical emplacement, the temperature gradients can be relatively high because the waste is emplaced comparatively close to the floor of the drift.

Some approximation or idealization is required when DOT is used to model the temperature conditions around a ventilated or unventilated drift. With DOT, special elements are available to handle prescribed, time-dependent, convective and radiative boundary conditions, but neither convective heat transfer within a material (e.g., air) nor radiative heat transfer between two surfaces can be modeled. Accordingly, the effect of the drift on the heat transfer in the rock has to be modeled either by prescribing a temperature at the drift wall boundary or by ascribing to the air in the drift thermal properties that approximate the effective of radiative and convective heat transfer.

The ventilated drift case can be treated by assuming that the effect of ventilation is to maintain a uniform wall temperature at all times. This is equivalent to assuming an unlimited supply of continuously cooled air, a condition that is poorly approximated in most underground excavations. However, if the wall rock temperature is selected judiciously, this approximation does provide a realistic amount of heat energy that will be removed by ventilating air, and, hence, the potential impact of ventilation on the drift behavior following waste emplacement.

A lower bound on the effect of ventilation can be provided by assuming that drifts are isolated from the repository ventilation system immediately after waste emplacement. To model this situation correctly, conductive, radiative, and

convective heat transfer within the drift should be considered. If, as in the present instance, only conductive heat transfer can be treated by the code used for analysis, then an approximate solution can be sought by assigning to the air within the drift an effective thermal conductivity.

In the investigation discussed here, two extreme ventilation conditions were considered. The temperature at the boundary of a ventilated drift was assumed to be maintained at 30°C(86°F), which is 7°C higher than the ambient conditions before disturbance by repository construction. For the unventilated drifts an effective thermal conductivity value of 50 W/m·K was used for the air drift. This value was selected so that the computed conductive heat transfer in the medium within the drift would approximate the combined effects of radiation, convection, and conduction that would be experienced in practice. Several investigators, including Buktovich and Montan (1980) and Sundberg and Eaton (1982), have discussed such an approximation and noted that the radiative heat transfer is the most important process. In summary, use of an effective radiation thermal conductivity (K_e) defined as follows is recommended:

$$K_e = 4\sigma T^3 L ,$$

In this equation σ ($5.6697 \times 10^{-8} \text{ W/m}^2 \cdot \text{K}^4$) is the Stefan-Boltzmann constant, T, the absolute temperature, and L, the average path length. A substitution of typical values for the absolute temperature and the drift dimensions leads to estimates for the effective radiation thermal conductivity in the range of 25 W/m·K to 100 W/m·K, depending on the values selected for the temperature and characteristic length.

To check on the sensitivity of the analysis to the assumed thermal conductivity of the air in the drift, three DOT analyses were performed using values of 25, 50, and 100 W/m·K. For these analyses the vertical emplacement method was used because the temperature gradients around the drift are much higher than those for the horizontal emplacement. In all cases the air was assumed to have a density of 1 kg/m³ and specific heat capacity of 1 kJ/kg·K, values the same as those used in all other calculations reported here. The results of these analyses, which indicated little sensitivity to the effective conductivity, are summarized in Table 7. All subsequent analyses were performed using 50 W/m·K.

3.5 Methods of Stability Evaluation

A conventional approach to the evaluation of the stability of underground excavations involves identifying possible modes of failure. In the present study, attention focused on two possible modes of failure in the tuff: rock matrix shear failure and slippage on pre-existing joints. In each case, the potential for failure at any point within the rock mass was assessed by calculating the ratio of the maximum allowable stress to the actual, computed stress. In this report the strength-to-stress ratio is sometimes referred to as the factor

of safety. It should be borne in mind, however, that this is a value calculated for a specific point within the rock mass and is not directly related to the stability of the entire excavation. On the other hand, if the results of such an evaluation indicate that an extensive region of rock around an excavation is subjected to stresses greater than can be sustained, stability of the excavation may be in doubt.

For the purposes of this report, it is assumed that the shear strength of the tuff rock matrix can be described using a linear Coulomb failure criterion. Specifically, if the computed major and minor principal stresses at a point in the plane of the section are σ_1 and σ_2 respectively, the factor of safety against matrix failure is defined by

$$FS_m = \frac{(\sigma_1 + \sigma_2)\sin\phi_m + \sigma_c (1 - \sin\phi_m)}{\sigma_1 - \sigma_2} \quad : \sigma_2 > \sigma_T,$$

in which σ_c and ϕ_m are, respectively, the uniaxial compressive strength and the friction angle for the matrix of the rock mass. (Values of these parameters are given in Table 3.) σ_1 and σ_2 are the major (more compressive) and minor (less compressive) principal stresses, respectively. If the minimum principal stress is less than the uniaxial tensile strength of the matrix (σ_T), the factor of safety is assumed to be zero.

The potential for activation of pre-existing joints, was evaluated with a methodology similar to that used for the unit evaluation of Yucca Mountain (Johnstone, Peters, and Gnirk, 1984). Specifically, the stress conditions along vertical joints were tested. It was assumed that the shear strength of such joints is defined by a Coulomb-Navier criterion. If σ_s and σ_n are the computed shear and normal stresses on a plane of a given orientation, the factor of safety against slip is defined by

$$FS_j = \frac{c_j + \sigma_n \tan\phi_j}{\sigma_s} \quad : \sigma_n > 0,$$

in which c_j and ϕ_j are, respectively, the cohesion and friction angle of the joint. (Values for these parameters are also given in Table 3). Because joints do not usually possess any strength in tension, the factor of safety is assumed to be zero if the normal stress, σ_n , is tensile. For the vertical joints tested in this study, σ_n is the horizontal stress. For the more general case, in which the joints are not vertical and do not strike parallel to the axis of the drift, transformation equations are required for calculating these values (Jaeger and Cook, 1969).

Finally, it is appropriate to reiterate that the results reported herein were all obtained using a linear elastic analysis technique. Plots of the strength/stress ratio, or factor of safety, whether for the rock matrix or the joints were obtained by processing the results of those linear analyses. No

attempt was made to simulate matrix failure or joint slip. Numerical modeling techniques for performing such simulations are available (see, for example, Thomas, 1980 and 1982). Their application was not considered necessary for these reference analyses since earlier studies indicate that the contribution of joint strain to the overall deformation around drifts in the Topopah spring tuff is small (Thomas, 1986) and no matrix failure was predicted by the present study. Because neither matrix failure nor joint slip were actually simulated during this study, the terms "potential failure" and "potential slip" are used in this report. Further, it should be noted that the analyses discussed here ignore any possible influence of support or reinforcement of the rock mass with rockbolts or other ground-control measures. Ground support will tend to reduce any predicted areas of overstress because of the confinement it provides to the rock mass.

4. ANALYSIS RESULTS

4.1 Vertical Emplacement

Analyses of the vertical emplacement drift were first performed using the HEFF boundary-element code. Results of these calculations are summarized in Table 8, in which closures, tangential stresses, and temperatures are listed for selected points on the drift boundary. The data are also presented in Figures 10 through 12.

The temperature, closure, and stress history plots reveal that the various quantities vary monotonically for approximately the first 100 yr after waste emplacement. Beyond that time all previous trends reverse. Hence, the results of the analyses of the drift immediately after excavation and 100 yr after waste emplacement give a good indication of the full range of response. The results of post processing data from the analyses of these two periods are illustrated in Figures 13 through 16.

Figure 13 illustrates the direction and magnitude of principal stresses around the drift. As elsewhere in this report, the "T" at the tip of a stress vector indicates tensile principal stress. It is noticeable that before waste emplacement the vertical stress at some distance from the drift boundary exceeds the horizontal stress. This reflects the assumption that the horizontal stress is initially 55% of the vertical, or overburden, stress. After waste emplacement, the horizontal stress increases steadily until it is several times greater than the vertical stress.

The consequences of the increase in the horizontal stress are illustrated in Figure 14, in which the distribution of tangential stress at the drift boundary is plotted. There is a very pronounced increase in the stresses in the roof and floor of the drift, and a small tensile stress is induced in the side walls. The latter may be attributed, in part, to a decrease in the vertical stress caused by the waste emplaced in other drifts, but is predominantly due to the

fact that the side wall bulges slightly into the drift as the horizontal loads increase.

The stability of the drift can be assessed by comparing the strength of the intact rock with the computed state of stress and by evaluating the importance of any zones where the stresses exceed the matrix strength, or where there is a potential for slippage of pre-existing joints. In Figure 15 the strength of the rock matrix (i.e., the intact, welded tuff) is compared with the stresses. Neither immediately after excavation, nor 100 yr after waste emplacement, is there any region where the stress exceeds the matrix strength. However, a decrease in the strength ratio is observable in the floor and the roof of the drift. The most severe conditions occur in the crown of the drift, where the strength ratio falls to approximately 1.25. The data presented in Table 8 are consistent with this finding because the predicted stresses at the boundary of the drift lie well within the range of 75.4 MPa to -9.0 MPa, which are, respectively, the estimated in-situ compressive and tensile strengths of the matrix (75.4 MPa is 50% of the value measured in laboratory tests of intact samples). Hence, based upon the assumptions inherent in the modeling, it appears that no stability problems associated with matrix failure are anticipated.

In Figure 16 the potential for slippage on a set of vertical joints is evaluated during excavation and for 100 yr after waste emplacement. At the later period there are small regions in the upper and lower portions of the drift boundary where the computed shear stresses exceed the shear strength. Inspection of the results of the calculations indicates that the shear stresses in the upper and lower lobes have opposite signs, indicating a potential for movement in opposite and counteracting directions. This fact also suggests that the magnitude of any shear displacement slippage would be small, if it were to occur. The shear stresses on vertical planes vanish at about midwall height, which is why the resistance to slippage is high in that region. The significance of these regions of overstress is discussed in greater detail in Section 5.

Figures 15 and 16 reveal that matrix overstress is more likely to occur in the crown and floor, whereas joint slippage is more likely in the side walls. Inspection of Figures 15 and 16 also indicates that the volume of overstressed rock is completely determined by the joint strength criterion. This is the situation in all cases analyzed during the study.

The results of the boundary-element calculations indicated that peak temperatures, stresses, and closure around the drift occur about 100 yr after waste emplacement, and that changes occur most rapidly at early times. For that reason, the thermal/mechanical finite-element analyses were performed for the period of excavation and for 10, 35, and 100 yr after waste emplacement. A summary of the results of the thermal analyses are shown in Tables 6 and 7.

The results of the finite-element analyses of the vertical emplacement drift, for both ventilated and unventilated conditions, are summarized in Table 9. Comparison of these results with those listed in Table 8 reveals that the boundary-element calculations and the finite-element analyses of the unventilated drift are generally in good agreement, particularly at early times. This is to be expected because heat transfer is predominantly through the rock mass, and there is no heat loss in the drift unless there is ventilation. There are substantial differences between the results of the finite-element analyses of the ventilated and unventilated vertical emplacement drifts. The analysis indicate that ventilation is effective in removing a significant proportion of the total heat generated by the emplacement waste. The effectiveness is attributed to the small standoff of the waste containers from the vertical emplacement drifts and to the close spacing of the drifts.

Figures 17 through 20 show the results of the finite-element analyses for ventilated and unventilated drifts: conditions immediately after excavation, as well as for 100 yr following waste emplacement are given. The source of the difference between the ventilated and unventilated cases can be immediately identified in Figure 17, which illustrates the temperature change in the rock mass 100 yr after emplacement. In the ventilated case, the drift boundary is fixed at 30°C, which is 7°C above the ambient rock temperature. This creates a high temperature gradient between the waste container and the drift boundary. Hence, the ventilating air removes a significant proportion of the thermal output of the waste containers. The resulting decrease in thermal stresses is illustrated in Figure 18, where it can be seen that the horizontal stresses midway between the adjacent drifts are approximately 50% higher than the initial stress when the drift is ventilated and five times higher when it is unventilated.

Plots of the matrix and joint strength/stress ratios are reproduced in Figures 19 and 20. There are marked differences between the ventilated and unventilated cases. However, the regions of overstress are still restricted to potential slippage of joints near the drift perimeter in the upper and lower portions of the drift wall. Once again, there is good agreement between the results of the finite-element analyses of the unventilated (Figures 19 and 20) drift and the results of the boundary-element analyses (Figures 15 and 16). Apparent differences may be attributed, very largely, to the fact that a much higher density of sample points was used in preparing the plots from the boundary-element analyses. Also, when the data from the finite-element analyses are contoured, only the values at the corner nodes of each element are used.

More complete output from the boundary-element and finite-element analyses of the vertical emplacement drifts is presented in Appendices A and B, respectively. The plots in Appendix B indicate that the stresses and temperatures within the interior of the rock mass begin to decrease some time earlier than 100

years after waste emplacement if the drift is ventilated. The peak values probably occur some time between 10 and 35 yr after waste emplacement: precisely when, and at what values, does not appear to be essential to the conclusions of this study. As illustrated by Figure 21, the region of overstress predicted for the vertical joint set remains relatively unchanged in the later years after waste emplacement.

4.2 Horizontal Emplacement

The results of boundary-element analyses of the horizontal emplacement drift are summarized in Table 10 and Figures 22 through 28. As for the vertical drift, the response appears to develop steadily over the first 100 yr. After that time the previous trends in temperature, stress, and closure reverse. Again, the changes occur relatively swiftly at early times, and the peak response is indicated at approximately 100 yr after emplacement.

The results of the boundary-element analyses of the horizontal emplacement drift immediately after excavation and 100 years after waste emplacement are reproduced in Figures 25 through 28. Again, the most obvious effect of thermal loading is to increase the horizontal stress severalfold. However, because of the greater standoff distance, the drift remains relatively cool, and there is a marked decrease in the vertical stress in the vicinity of the drift. In contrast to the vertical emplacement drift, the horizontal emplacement drift is well adapted to the revised stress state. This is reflected in the more moderate values of the boundary stresses seen in Figure 24 (refer also to Figure 12).

The plots of the strength/stress ratios for the horizontal emplacement drift are reproduced in Figures 27 and 28. Once again, as indicated by data reproduced in Table 10, the compressive and tensile stresses are significantly lower than the corresponding strengths through the first 200 yr following waste emplacement. Behavior very similar to that of the vertical emplacement drift is observed, with potential joint slippage restricted to relatively shallow regions near the upper and lower portions of the boundary of the drift. Again, joints appear to play an important role only in the walls of the drift. Remote from the drift, as well as in the roof and floor, the shear strength of the vertical joints is increased by the thermally induced, horizontal stress.

The results of the finite-element analyses of the horizontal emplacement drift are summarized in Table 11 and illustrated in Figures 29 through 32. The temperature plots in Figure 29 reveal some differences between the ventilated and unventilated cases, but these are far less marked than those of the vertical emplacement drifts. This is reflected by the fact that the principal stresses in the vicinity of the drift, illustrated in Figure 30, are similar in the two cases. The ventilation does little to relieve the thermally induced, horizontal stress, but cooling does result in a local reduction of the vertical stress. As may be observed in Figures 31 and 32, this reduction in vertical stress has

little impact on the computed stress/strength ratio because these are predominantly controlled by the horizontal stress.

More complete output from the boundary-element and finite-element analyses of the horizontal emplacement drifts is presented in Appendices C and D, respectively. In view of the fact that the heat removed from the drift through ventilation is relatively modest, the peak stresses and temperature in the vicinity of the drift occur at much later times than for the vertical emplacement scheme. Accordingly, the plots presented in this section appear to adequately represent the range of conditions that may be expected in the vicinity of the drift during the first 100 yr following waste emplacement.

5. DISCUSSION

The primary objective of the analyses documented by this report was to provide a consistent set of predictions of the thermal/mechanical response of the emplacement drifts for the current designs for vertical and horizontal emplacement of nuclear waste. This objective has been met by presenting data, in tabulated and graphical form, that provides detailed information on the effects of initial excavation and conditions during the first 200 yr after waste emplacement. Analyses of continuously ventilated and entirely unventilated drifts were performed because these conditions represent reasonable extremes of those that might be adopted in a repository.

As illustrated by data presented in Section 4 and by Figures 33 and 34, the predictions made using boundary-element and finite-element models are in good agreement, when the effect of ventilation is ignored. This measure of agreement increases confidence in the results and has provided a measure of verification of all computer codes used in the study. Additionally, it confirms the usefulness of the boundary-element codes for conducting scoping analyses of stress-related effects since the unventilated case provides the more severe stresses. The results of the analyses have also provided a basis for assessing the suitability of the current designs of the emplacement drift for a repository in tuff.

If the results of the analyses are reviewed, two important features may be noted. These are, namely, that the effect of waste emplacement is to increase, temporarily, the horizontal stresses to which the rock mass is subjected; and, that the response to thermal loading can be very sensitive to how, if at all, the repository is ventilated after the waste is emplaced. These effects are illustrated in Figures 35 and 36 by the temperature and horizontal stress histories for points on the repository horizon, approximately 17.5 m from the centerline of the drifts. For the vertical emplacement drift, these histories are representative of conditions in the center of the pillar between adjacent drifts. For the horizontal emplacement drift they would be representative of a point midway between the drift and the first container in the emplacement hole.

The effect of the high levels of horizontal stresses is to induce high levels of stress in the roof and floor of the drifts (see Figures 14 and 26) and to cause the sidewalls to displace inward (Figures 33 and 34). The latter condition is accompanied by the development of tensile stresses in the sidewalls. These would result in either the opening of any pre-existing, near-horizontal joints or the formation of new horizontal fractures in a small region near the openings, if the matrix tensile strength were exceeded. However, the results of analyses do not indicate that stresses in the vicinity of the drift ever exceed either the compressive or tensile strength of the rock matrix. On the other hand, the movement of the sidewalls into the drift does result in the development of shear stresses that exceed the assumed shear strength of vertical joints. The origin of this behavior is illustrated in Figure 37. The behavior is observed for both the vertical and horizontal emplacement drifts, but conditions for the latter appear preferable because the shape is intrinsically better suited to withstand high levels of horizontal stress. The regions of overstress extend no deeper than 1 m into the wall and are considered benign because only a few joints are expected to be affected, and because it is kinematically impossible for any significant shear displacement to occur along these surfaces. In fact, as is illustrated in Figure 37, shear displacements on joints in the upper and lower portions of the walls of the drifts are in opposing directions.

The effect of repository ventilation is particularly striking with respect to the vertical emplacement option. This is not surprising, as substantial portions of the thermal energy released by the waste will be removed if excavations close to the waste are ventilated continuously. In the present instance, no estimate of the heat load to the ventilation system was made, but recent thermal calculations for a different vertical emplacement design indicated that 10 yr after emplacement, approximately 60% of the instantaneous thermal output of the waste would be removed by ventilation (St. John, 1985).

The range of ventilation conditions investigated in this study represents two extremes, neither of which are completely practical. Drifts will certainly be ventilated during construction and emplacement, and continuous ventilation to maintain a wall temperature of 30°C would be unnecessary to ensure an acceptable working environment. The actual conditions will, therefore, lie somewhere between the two extremes considered in this report. As a consequence, on the basis of results presented here, it can be stated that ventilation will have a moderating effect on the results of waste emplacement, but it is not of critical concern. Even without ventilation, the horizontal emplacement option meets the design criterion (Mansure and Stinebaugh, 1985) that the temperature not significantly exceed 50° in 50 years (refer to Figure 10). The question of whether sudden ventilation of a previously unventilated (or sparingly ventilated) drift may adversely affect stability has been addressed in another investigation. It was concluded that there was no evidence that stability problems would be accentuated by so-called blast cooling (Svalstad and Brandshaug, 1983).

The results of simple linear analyses of the type presented in this report provide no direct measure of the stability of underground excavations. However, in the present instance, they provide useful data on how conditions may change after excavation, and this information can be used to assess potential behavior. Specifically, it is observed that the horizontal stress may increase fivefold (Figure 36) if there is no ventilation, but that there are only minor changes in the vertical stress. The practical implication of these changes is most conveniently discussed in terms of potential failure mechanisms.

Two types of failure are commonly observed in underground excavations. The first is the instability of the rock in the immediate vicinity of the excavation. This may be progressive and eventually lead to complete loss of utility if the ground support is inadequate. The second type of failure is peculiar to situations, such as extensive underground mining of a coal seam or orebody, where the rock remaining between excavations (commonly known as pillars) is overloaded. This second type of failure is inconceivable in a nuclear waste repository because the amount of rock removed is very small, even for the vertical emplacement option, and the vertical stresses remain essentially constant despite waste emplacement. (This statement is supported by the high strength/stress ratios for the rock matrix outside the immediate vicinity of the drift, which are illustrated throughout this report.)

Attention must, therefore, focus on potential failure around the drift. In this case several possible failure mechanisms might be considered. Those typical of excavations in a jointed rock mass are gravity falls of blocks from the roof and side walls, and spalling and slabbing. Typically, any blocks are defined by pre-existing fractures. In welded tuff the joints are predominantly vertical, and there are few horizontal or subhorizontal joints or other fractures. Hence, the likelihood of the development of large, potentially unstable blocks of rock in the roof of the drifts is considered small. Also, even with drift ventilation, the shear strength of the joints in the roof of the drift will be high because of the relatively high, horizontal stress levels. The movement of slabs of rock, formed by subvertical joints, may be observed in the sidewalls, but these will be quite shallow and are normally controlled by rockbolting or other rock-support measures. Therefore, it is concluded that any gravity-induced failure is likely to be very superficial and would be adequately counteracted by normal ground support and routine maintenance.

Spalling and slabbing around underground excavations is seldom observed in more massive rocks when the regional stresses in the vicinity of the drift are less than one-fifth of the uniaxial compressive strength of the rock (Hoek and Brown, 1980). For the present analyses, the matrix strength of the rock was estimated to be 75.4 MPa. The predicted peak horizontal stresses to which the emplacement drifts are subjected following waste emplacement lie in the range of 10-15 MPa in the absence of ventilation (Figure 36). Hence, empirical evidence suggests that there might be some minor slabbing but not major failure in regions

where joints in the tuff rock mass are widely spaced. More likely, however, there will be a sufficient number of joints that any potential for stress-induced spalling or slabbing is reduced. In any event, failure is most likely to be superficial and should be handled by normal support and maintenance.

In conclusion, it appears reasonable to assert that the analyses documented herein provide an adequate description of temperature and stress changes around excavations for vertical or horizontal emplacement of radioactive waste. Design details have changed since the completion of these analyses, but the basic concepts remain the same and results of analyses of the current conceptual design would be similar to those presented here providing the thermal loading is equivalent. The results of the analyses have provided evidence that the drifts in the Nevada Test Site will be stable under the set of conditions expected for drifts in Yucca Mountain. This finding is consistent with the conclusions of earlier studies performed as a part of the process of selection of the Topopah Springs members as the candidate horizon for repository construction (Johnson, 1986; Johnstone, Peters and Gnirk, 1984; and Thomas, 1986). Of the two emplacement options, the horizontal appears to be better suited to withstand the high horizontal stress levels that are the inevitable consequence of radioactive waste emplacement. It is recognized that actual conditions could deviate from those modeled in this study, but the accuracy of those predictions is considered to be consistent with the present level of understanding of the repository layout and the material properties of the candidate horizon for repository construction. Confirmatory evaluations in the planned exploratory shaft test facility in Yucca Mountain are deemed warranted to assess the usefulness of the models employed within this and similar studies, and the database supporting them.

REFERENCES

- Bauer, S.J., F. J. Holland, and D.K. Parrish, "Implications about In Situ Stress at Yucca Mountain," 26th U.S. Symposium on Rock Mechanics, Rapid City, SD, June 1985.
- Brady, B.H.G., "HEFF, A Boundary-Element Code for Two-Dimensional Thermoelastic Analysis of a Rock Mass Subject to Constant or Decaying Thermal Loading," User's Guide and Manual, RHO-BWI-C-80. Prepared by the University of Minnesota for Rockwell Hanford Operations, Richland, WA, June 1980.
- Buktovich, T.R. and D.N. Montan, "A Method for Calculating Internal Radiation and Ventilation with the ADINA Heat Flow Code," UCRL-52918, Lawrence Livermore Laboratory, Livermore, CA, April 1980.
- Crouch, S.L and A.M. Starfield, Boundary-Elements Methods in Solid Mechanics, George Allen and Unwin, London, 1983.
- Davis, S.N. and R.J.M. DeWiest, Hydrogeology, John Wiley and Sons, New York, 1966.
- DOE (U.S. Department of Energy), "Site Characterization Plan for Yucca Mountain Site," Office of Civilian Radioactive Waste Management, Washington, D.C. (in preparation).
- DOE (U.S. Department of Energy), "Generic Requirements for a Mined Geologic Disposal System, Appendix B," ORG/B-2, September 1984.
- Eglinton, T.W. and R.J. Dreicer, "Meteorological Design Parameters for the Candidate Site of a Radioactive Repository at Yucca Mountain, Nevada," SAND84-0440/2, Sandia National Laboratories, Albuquerque, NM, 1984.
- Hoek, E. and E.T. Brown, Underground Excavations in Rock, Institution of Mining and Metallurgy, London, 1980.
- Jaeger, J.C. and N.G.W. Cook, Fundamentals of Rock Mechanics, Methuen and Company, Limited, London, 1969.
- Johnson, R.L., "NNWSI Unit Evaluation at Yucca Mountain, Nevada Test Site: Near Field Thermal and Mechanical Calculations Using the SANDIA-ADINA Code," SAND83-0030, Sandia National Laboratories, Albuquerque, NM, 1986.
- Johnstone, J.K., R.R. Peters and P.F. Gnirk, "Unit Evaluation at Yucca Mountain, Nevada Test Site: Summary Report and Recommendations," SAND83-0372, Sandia National Laboratories, Albuquerque, NM, June, 1984.
- Lindner, E.N., C.M. St. John, and R.D. Hart, "A User's Manual and Guide to SALT3 and SALT4: Two-Dimensional Computer Codes for Analysis of Test-Scale Underground Excavations for the Disposal of Radioactive Waste in Bedded Salt Deposits," ONWI-145, Office of Nuclear Waste Isolation, Battelle Memorial Institute, Columbus, OH, February, 1984.
- MacDougall, H.R. (Compiler), "Site Characterization Plan Conceptual Design Report," Draft SAND84-2641, Sandia National Laboratories, Albuquerque, NM, November, 1986.
- Mansure, A.J., "Allowable Thermal Loading as a Function of Waste Age," Letter Report to R. Hill, February 13, 1985, Division 6314, Sandia National Laboratories, Albuquerque, NM.
- Mansure, A.J. and T.S. Ortiz, "Preliminary Evaluation of the Subsurface Area Available for a Potential Nuclear Waste Repository at Yucca Mountain," SAND84-0175, Sandia National Laboratories, Albuquerque, NM, December 1984.

Mansure, A.J. and R.E. Stinebaugh, "Memorandum of Record of Instructions for Thermal Design Analysis and Performance Assessment of Layout," Version 1, Letter Report to R. Hill, Division 6314, Sandia National Laboratories, Albuquerque, NM, April 18, 1985.

Nimick, F.B., S.J. Bauer and J.R. Tillerson, "Recommended Matrix and Rock Mass Bulk, Mechanical and Thermal Properties for Thermomechanical Stratigraphy of Yucca Mountain," Version 1, Keystone Document Number 6310-85-1, Sandia National Laboratories, Albuquerque, NM, October 1984

ONWI (Office of Nuclear Waste Isolation), "DOT: A Nonlinear Heat Transfer Code for Analysis of Two-Dimensional Planar and Axisymmetric Representations of Structures," ONWI-420, Battelle Project Management Division, Columbus, OH, April 1983a.

ONWI (Office of Nuclear Waste Isolation), "VISCOT: A Two-Dimensional and Axisymmetric Nonlinear Transient Thermoviscoelastic and Thermoviscoplastic Finite-Element Code for Modeling Time Dependent Viscous Mechanical Behavior of a Rock Mass," ONWI-437, Battelle Project Management Division, Columbus, OH, April 1983b.

Owen, D.R.J. and E. Hinton, Finite Elements in Plasticity: Theory and Practice, Pineridge Press, 1980.

Parsons, Brinckerhoff, Quade and Douglas, "Nuclear Waste Repository in Tuff Subsurface Facility," Sandia National laboratory Drawing Nos. R06916, R07015, R07020, R07021, R07024, R07037, 1986.

Polivka, R.M. and E.L. Wilson, "Finite-Element Analysis of Nonlinear Heat Transfer Problems," UC SEM 76-2, Department of Engineering, University of California, Berkeley, CA, 1976.

Sass, J.H. and A.H. Lachenbruch, "Preliminary Interpretation of Thermal Data from the Nevada Test Sits," USGS Open-File Report 82-973, 1982.

✓ St. John, C.M., "Investigative Study of the Underground Excavations for a Nuclear Waste Repository in Tuff." SAND83-7451, Sandia National Laboratories, Albuquerque, NM, April 1987 (in preparation).

✓ St. John, C.M., "Thermal Analysis of Spent Fuel Disposal in Vertical Emplacement Boreholes in Welded Tuff Repository," SAND84-7207, Sandia National Laboratories, Albuquerque, NM, September 1985.

Sundberg, W.D. and R.R. Eaton, "Three-Dimensional Thermal Analysis for a Conceptual High Level Repository in Welded Tuff," SAND81-0215, Sandia National Laboratories, Albuquerque, NM, April 1982.

Svalstad, D.K. and T. Brandshaug, "Forced Ventilation Analysis of a Commercial High-Level Nuclear Waste Repository in Tuff," SAND81-7206, Sandia National Laboratories, Albuquerque, NM, June 1983.

Thomas, R.K., "NNWSI Unit Evaluation at Yucca Mountain, Nevada Test Site: Near Field Mechanical Calculations Using a Continuum Jointed Rock Model in the JAC Code," SAND83-0070, Sandia National Laboratories, Albuquerque, NM, 1986.

Thomas, R.K., "A Material Constitutive Model for Jointed Rock Mass Behavior," SAND80-1418, Sandia National Laboratories, Albuquerque, NM, November 1980.

Thomas, R.K., "A Continuum Description for Jointed Media," SAND 81-2615, Sandia National Laboratories, Albuquerque NM, April 1982.

Zeuch, D. and E. Eatough (Compilers) "Reference Information Base for Nevada Nuclear Waste Isolation Project," SLTR86-5005, Sandia National Laboratories, Albuquerque, NM, 1986.

Zienkiewicz, O.C., The Finite-Element Method in Engineering Science, McGraw Hill, London, 1977.